Hindawi
Advances in Civil Engineering
Volume 2021, Article ID 8869198, 14 pages
https://doi.org/10.1155/2021/8869198

Research Article

Numerical Analysis of Two I-shaped GFRP Composite Bridge with Corrugated Webs

Linjun Yan,[1] **Jingwei Zhang**,[1] **and Kui Luo**[2]

[1]*College of Civil Engineering, Lanzhou Jiaotong University, Lanzhou 730070, Gansu, China*
[2]*College of Civil Engineering, Hunan University, Changsha 410082, Hunan, China*

Correspondence should be addressed to Linjun Yan; yanlj@mail.lzjtu.cn

Received 4 August 2020; Revised 6 December 2020; Accepted 29 December 2020; Published 1 February 2021

Academic Editor: Claudio Mazzotti

With the advantage of high strength, lightness, and good environmental resistance, glass fiber reinforced polymer (GFRP) pultruded profile is regarded as an innovative way that has been used in infrastructure over the last few decades. However, some disadvantages also limited its widespread application in practice, including relatively low elastic and shear modulus and high deformability due to buckling failure. To overcome these disadvantages, some composite structure systems are proposed, such as GFRP-concrete composite structure system. This paper presents an innovative GFRP-concrete composite bridge prototype system, which mainly includes two I-shaped GFRP girders with corrugated webs combined with a thin steel fiber reinforced self-compacting concrete (SFRCC) deck. This composite bridge system is proved to improve structure shear stability and bending stiffness. Three-dimensional finite element (FEA) models are created to simulate the flexural behavior of two-I-shaped-girder composite bridge with straight webs, and the model result is validated with experimental data. Furthermore, the revised FE model that uses corrugated webs instead of straight webs is created, and the static and dynamic behaviors are investigated, including shearing stability properties, bending vibration frequency due to bending and torsion, mid-span vertical deflection, and lateral displacement due to wind load. Further research efforts on the influence of parameters dimension variation in corrugated webs girder composite system are needed. A total of four variable parameters are selected to test, which are GFRP corrugated web width, thickness, height, and SFRCC top slab thickness, respectively. All these conclusions will provide some design recommendations and guideline of a GFRP-concrete corrugated webs composite bridge in further study.

1. Introduction

Compared with traditional construction materials, fiber reinforced polymer (FRP) materials have been increasingly used in infrastructure applications, due to its beneficial material properties. These advantages include relatively low self-weight, good environmental resistance, high strength-to-weight ratios, and nonmagnetic properties, etc. [1, 2]. Compared with other FRP materials, glass fiber reinforced polymer (GFRP) exerts higher demand because of relatively reasonable cost and stable performance [3]. Recently, several researchers investigated GFRP in manufacturing composite slab [4], FRP composites jacket [5], and other hybrid structures [6]. Pultruded GFRP profiles greatly improved structure capacity and environmental durability, and it is considered as one of promising applications in structure engineering [7]. In addition, GFRP girder in the composite system is manufacturer prefabrication, which significantly shortened the construction period when compared with the conventional construction. Some designers attempt to use GFRP profiles in bridges and buildings, but high deformability and susceptibility to instability phenomena always limit its full exploitation [8–10]. To overcome these limitations, composite structural systems have been proposed using their advantages to make up for deficiencies, like GFRP-concrete composite system. It should be noted that GFRP pultruded profiles combined with concrete compression elements can increase flexural stiffness and structure strength and make a better use of GFRP profiles to prevent the occurrence of instability phenomena. Additionally, the cross-sectional redundancy leads to a certain pseudo-ductility in composite systems when compared with

the common fragile failure mechanisms of simple GFRP profiles [11]. Fardis and Khalili [12] firstly proposed GFRP-concrete composite system that included concrete-filled rectangular GFRP box sections with an open top for beams. Fam et al. [13] tested rectangular concrete-filled FRP tubes (CFFTs) in bending, where GFRP tubes were either entirely filled with concrete or partially filled by having an inner hole. Fam and Honickman [14] investigated a new built-up box girder that consisted of a trapezoidal hat-shaped GFRP section and a top flat GFRP plate, supported by a cast-in-place concrete slab. Nowadays, a GFRP-concrete composite prototype is gradually suitable for bridge engineering with the development of easy and quick installation technology. Some lab experiments have been conducted by two I-shaped GFRP girders with a thin steel fiber reinforced self-compacting concrete (SFRCC) deck, as shown in Figure 1.

Correia et al. [15, 16] evaluated the flexural behavior of GFRP I-profile concrete composite beams and firstly used the shear connection on GFRP I-profile, which connected top concrete slab with stainless steel bolts. They also studied the flexural behavior of multi-span GFRP-concrete composite beams, with the shear connection provided by a continuous epoxy adhesive layer. Mendes et al. [17] assessed adhesively bond behavior between GFRP girder and SFRSCC when subjected to fatigue loading and severe environmental condition. Gonilha et al. [18–20] investigated the integral work performance of a GFRP-concrete composite footbridge, and an 11.0 m length GFRP-SFRSCC composite footbridge was tested to study the practical feasibility and its manufacturing and assembly process. To consider dynamic response under pedestrian loads, Gonilha et al. [21, 22] used push-out tests to analyze a footbridge prototype comprising GFRP pultruded profiles and thin SFRSCC precast concrete slabs. Creep behavior of GFRP-concrete composite structures was monitored and long-term deformation of this type structures was predicted. Sause and Braxtan [23] discussed that GFRP corrugated webs are used in composite concrete girder, which have higher shear buckling strength than the straight webs. The impact behavior, damage modes, and energy dissipation of the hybrid corrugated web were studied and the residual load carrying capacity after impact was investigated using four-point bending test [24]. To improve structure shear stability, two I-shaped composite girders with GFRP corrugated webs instead of straight webs are proposed, as shown in Figure 2.

Finite element analysis (FEA) modeling is applied in this paper to investigate the mechanical performance of newly proposed girder and includes three-step analysis process. Firstly, the original girder type, which is two I-shaped GFRP with straight webs-concrete composite system, is modeled and calibrated by existed experimental research. Secondly, the straight webs are replaced by corrugated webs to form new proposed girder type, which is two I-shaped GFRP with corrugated webs-concrete composite system. FEM method is used to model and investigate the mechanical performance. Finally, a parametric study is predicted in the new proposed FEA model, such as the shear buckling stability, dynamic characteristics, deflection under serviceability load, and lateral displacement due to wind load.

2. Experimental Program

2.1. Characteristics of Two I-Shaped GFRP Girders with Straight Web Composite Bridge Prototype. Gonilha et al. [18, 19] used an experimental test to study the dynamic properties and flexural behavior of a total length of 6.0 m (span length is 5.5 m) footbridge, using prototype of two I-shaped GFRP-concrete composite girders with straight webs. The composite girder comprises two I-shaped pultruded profiles with straight webs (200 mm height by 100 mm width by 10 mm thickness), and a thin precast slab on top using SFRSCC deck (2000 mm width by 40 mm thickness). The connection between the GFRP web and the SFRSCC deck used 2 mm thickness epoxy adhesive layer and combined with M10 stainless steel bolts. This shear connection is considered as a linear elastic relationship. Table 1 shows geometric parameters dimension of composite girders system, and the introduction of each parameter is indicated in Figure 1.

For boundary condition, support on the left side is defined as pinned, where horizontal displacement, vertical displacement, and longitudinal rotation are restraint. Support on the right side is defined as a roller, and only vertical displacement is restraint. Concrete jackets are cast between the top and bottom flanges in both ends, as shown in Figure 3. Secondary girder exists at the location of support and mid-span sections, which is used to connect the two main girders, as shown in Figure 4.

2.2. Material Properties. Generally, two-I-shaped GFRP-concrete composite girder system includes four main physical elements: GFRP pultruded girder, SFRSCC concrete deck, epoxy adhesive, and stainless steel anchors. All these material properties are derived from experimental testing and manufacturer. The GFRP pultruded profiles are made of roving and E-glass fibers, embedded into isophthalic polymer resin matrix. Based on the manufacturer code, the GFRP laminates material properties (for GFRP girder web and flange) are obtained, which include longitudinal elasticity modulus in tension ($E_{L,t}$), transverse elasticity modulus in compression ($E_{T,c}$), in-plane shear modulus ($G_{L,t}$), longitudinal tensile strength ($f_{tu,L}$), and in-plane shear strength ($\tau_{tu,\ L}$), as shown in Table 2. Similarly, SFRSCC concrete deck material properties are determined by experimental testing, and listed as follows: (i) elasticity modulus ($E_{c,\ 28} = 36.97 \pm 1.94$ GPa); (ii) Poisson ratio ($\nu = 0.33 \pm 0.03$) in compression; (iii) splitting tensile strength ($f_{cr} = 9.42 \pm 1.63$ MPa); (iv) compressive strength ($f_{cm} = 80.65 \pm 2.07$ MPa); and (v) volumetric weight ($\rho = 24.0$ kN/m^3). The epoxy adhesive is mainly used to connect GFRP girders and SFRSCC deck, and material properties include tension elasticity modulus ($E_a = 8.8$ GPa) and tensile strength ($f_{au} = 17.3$ MPa). The additional connection between main and secondary girders is stainless steel anchors, which materialized by $M10 \times 55$ with a bearing capacity of $f_{bk} = 700$ MPa.

2.3. Experimental Test Preparation. The experimental program includes GFRP-concrete composite girder footbridge 4-point (two supports and two load points) bending quasi-

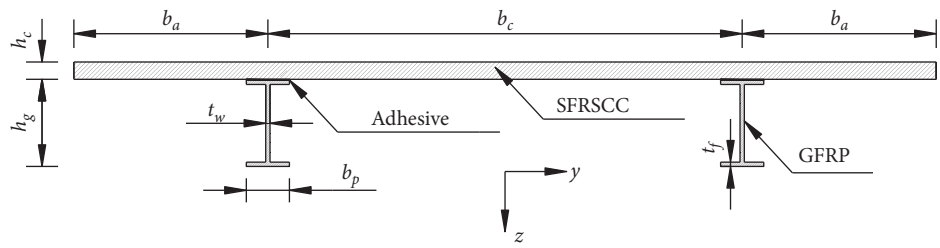

Figure 1: Cross-section of the two I-shaped GFRP with straight webs-concrete hybrid girder.

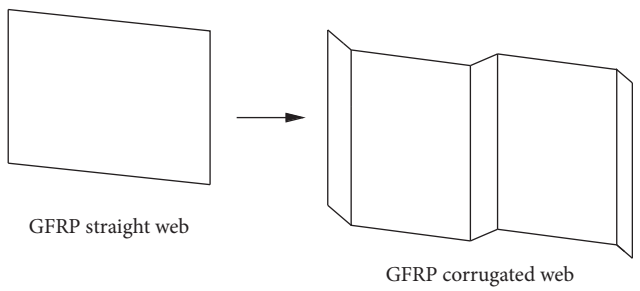

Figure 2: Comparison between GFRP straight web and GFRP corrugated web.

Table 1: Geometric parameters of the hybrid girder (mm).

h_g	b_p	b_a	b_c	t_w	t_f	h_c
200	100	450	1100	10	10	40

static flexural test, and two static loads are applied for two rectangular concrete blocks to build a two-point loading configuration, as shown in Figure 3. Each of the rectangular blocks has dimensions of 1.20 m long by 0.20 m wide, as shown in Figure 5. The block self-weight is approximately 640 kgf (total load, $F = 12.56$ kN), which corresponds to approximately 23% of the typical load defined in Eurocode (5 kN/m^2 for footbridge structures in the entire deck) [25]. The spacing between two load points is 1.70 m, and the distance from load point to nearest support point is 1.90 m. The distance of 0.25 m is measured from footbridge end to support point on both sides. The dynamic behavior of the GFRP-concrete composite girder footbridge is investigated, which includes natural frequencies, mode shape, and damping ratio. Vertical and transverse structural accelerations are also measured with a time interval of 5 min, using a rubber hammer knocking on the deck to simulate random impact loads.

3. Numerical Modeling Validation Test

A three-dimensional FEA model using ANSYS is conducted to predict the mechanical behavior of the GFRP-concrete composite girder footbridge. Figure 6 shows the simulation of a footbridge with GFRP straight webs in the longitudinal direction, and three types of model elements are used, which include solid element, shell element, and two-joint rigid link element, respectively. The 3D solid (SOLID45) element is used to simulate SFRSCC concrete slab, epoxy adhesive layer, and concrete jackets, respectively. The shell (shell 63) element is used to simulate GFRP girder flange and web. The two-joint rigid link element is used to simulate stainless steel anchor bolts, which are used to connect main and secondary girders. The connection between GFRP girder flanges and web also uses rigid link element. The boundary conditions use stiff springs (stiffness equals 3.5×10^6 kN/m) and set up support rotation center alignment. For material properties of structure member, the GFRP girder is modeled as orthotropic materials, while the SFRSCC concrete slab and the epoxy adhesive are modeled as isotropic materials. A linear elastic relationship is considered for all materials and analysis process, and damping coefficients are determined by modal analysis.

The static behavior of mid-span deflection and neutral axis position are monitored in numerical FEA model and compared with experimental test, which is summarized in Table 3.

Based on the comparison result, Figure 7 shows that the FEA model maximum deflection relative error rate is 6% when compared with lab test data and leads to slightly elevated neutral axis position. The unequal deflection can be explained as a geometric irregularity during the construction and the presence of micro-cracks on SFRSCC concrete deck surface, caused by concrete creep and shrinkage phenomenon. Figure 8 shows force-strain development trend in girder top, middle, and bottom location with respect to experimental data and FEA model, respectively. Both methods' data show a nearly identical linear increase trend for all force-strain relations, which results in failure load of 200 kN and maximum strain values from girder top to bottom of 0.0011, 0.0038, and 0.0072, respectively. It can be concluded from all these observations that FEA model simulated mid-span deflection results have a good agreement with experimental test data, and the static FEA modeling accuracy is validated.

In order to understand the dynamic behavior of footbridge with straight webs, a dynamic model calibration test is carried out to estimate the mode shapes and natural frequencies. The first four vibration mode shapes are shown in Figure 9, and model simulation result is in good agreement with experimental test data, derived from [18]. In addition, the mode vibration frequencies between FEA model and experimental test are compared and summarized in Table 4, in which mode shapes 1 and 3 are for flexural vibration, and mode shapes 2 and 4 are for torsional vibration. The differences between numerical and experimental test frequencies values are 2.7%, 1.3%, 5.1%, and

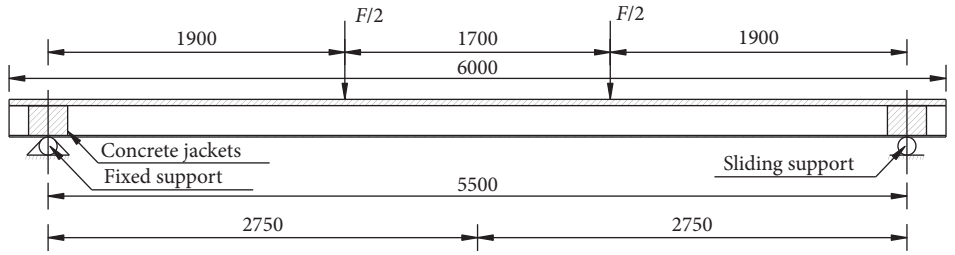

Figure 3: Side view of the GFRP-concrete hybrid structure (mm).

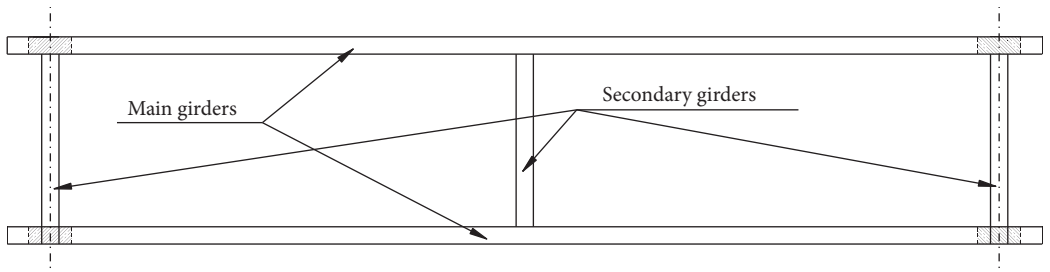

Figure 4: Bottom plan view of the GFRP-concrete hybrid structure.

Table 2: Main properties of the GFRP pultruded profiles.

GFRP	$E_{L,t}$ (GPa)	$E_{T,c}$ (GPa)	$G_{L,t}$ (GPa)	$f_{tu,L}$ (MPa)	$\tau_{tu,L}$ (MPa)	ρ (kN/m^3)
Webs	32.85 ± 1.09	5.74 ± 0.73	3.51 ± 0.24	376.69 ± 7.44	24.34 ± 0.86	18.0
Flanges	35.94 ± 2.35	4.35 ± 0.93	—	410.67 ± 18.60	—	18.0

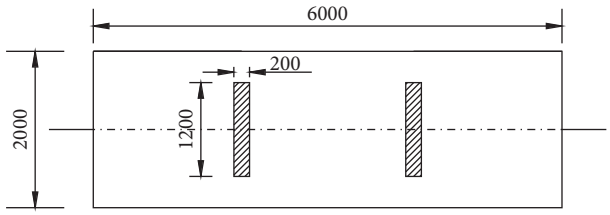

Figure 5: Loading deck area (mm).

5.4%, respectively. The second torsional vibration has a relatively higher error rate (5.4%), which may be caused by the higher stiffness of FEA model rigid link element between main and secondary girders. It can be concluded that the proposed FEA model has a good accuracy to predict vibration mode shapes and vibration frequency values. All conclusions mentioned above confirm that the proposed FEA model simulation can efficiently simulate the static and dynamic behavior of a hybrid GFRP-concrete prototype.

4. Numerical Modeling of GFRP Girder with Corrugated Webs

4.1. Static and Dynamic Model Analysis for GFRP Girder with Corrugated Webs. The previous FEA model for two I-shaped GFRP-concrete composite girders with straight webs is already validated by the experimental test data. Thus, new proposed FEA model is presented, which uses GFRP corrugated webs instead of the straight webs in the previous FEA model and all others keep its default, as shown in Figure 10.

The maximum advantage of GFRP corrugated webs is an obvious improvement in shear capacity when compared with the same dimension of the straight webs. Figure 11 shows a typical GFRP corrugated web detail information with one wavelength, in which A ($A = 25$ mm) is the flat length of GFRP corrugated web, B and C ($B = C = 27$ mm) are the inclined lengths of GFRP corrugated web, t_w ($t_w = 10$ mm) is the thickness of the GFRP corrugated web, and GFRP corrugated web width is 10 mm.

SFRSCC concrete slab, epoxy adhesive, and stainless-steel anchors simulation are identical to the previous straight web FEA model. The static (mid-span deflection and neutral axis position) and dynamic (mode shape and frequency) behavior of GFRP girder with the corrugated webs are compared with straight webs model, and the results are summarized in Tables 5 and 6, respectively.

It is worth noting that variation of web shape has not changed the order of vibration mode shape. Table 5 lists the frequencies of bending and torsion mode shape comparison result for corrugated and straight webs FEA model. It can be observed that all frequency values are decreased to a certain degree when the corrugated web model is used, but it is not a significant variation (mode 1: −6.6%; mode 2: −2.2%; mode 3: −5.5%; mode 4: −2.5%). Flexural vibration exerts a faster decline trend than torsional vibration. It can be explained

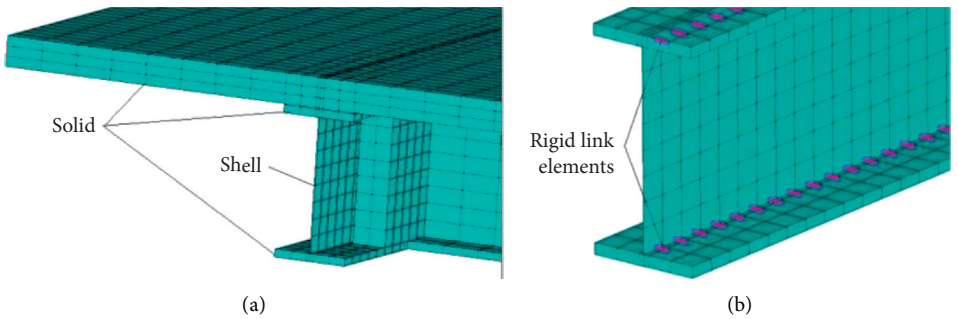

Figure 6: Finite element model and rigid connections of the GFRP-concrete hybrid girder. (a) 3D finite element model. (b) Detail of rigid connections.

Table 3: Comparison the mid-span deflection and neutral axis position of test girder between the FE values and measured values.

Static test	FE model	Experimental
Mid-span average deflection (mm)	7.24	6.79
Neutral axis position (mm)	31.19	24.55

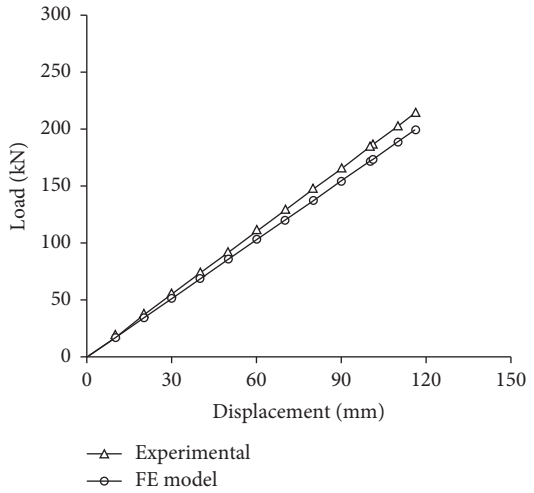

Figure 7: Failure test: mid-span deflections up until failure. Experimental tests and numerical predictions.

that corrugated webs model exhibits lower torsional stiffness and bending stiffness than those of the straight webs model. Furthermore, bending stiffness shows relatively steep descent trend, which may vary due to the physical dimension variation (like corrugated web width, corrugated web thickness, etc.). The displacement contours of the two FEA models are presented in Figure 12. The corrugated webs model vertical deflection distribution is similar to straight webs model, but the maximum value increases 14%, as shown in Table 6 and Figure 11. It can be explained that corrugated web transverse stiffness is lower than the straight web, which causes decreasing of restraint rigidity. Beyond that, the mid-span moment results in an increase in accord with decreasing of self-control, which ultimately leads to ascending of vertical displacement and variation of neutral axis position.

In order to investigate the effect of GFRP corrugated web width, five different web widths are necessary to select, which are 10 mm, 15 mm, 20 mm, 25 mm, and 30 mm, respectively. With increasing of corrugated web width in composite girder system, the buckling performance is significantly improved and leads to the buckling load linearly increasing 1.09 times, 1.14 times, 1.19 times, 1.23 times, and 1.26 times, respectively. It can be explained that web width variation directly influenced slant angle of corrugated web, which contributes to improving buckling load capacity. SFRSCC concrete deck is designed for compression member and used to resist flexural strength in GFRP-concrete composite girder system. Thus, it is apparent to state that the replaced corrugated webs show a slowly descending trend in bending and torsional stiffness, but the main responsibility of shear stability has a significant improvement.

4.2. Dynamic Parameters Analysis for GFRP Girder with Corrugated Webs. In order to study the dynamic behavior of GFRP girder with corrugated webs, four physical parameters

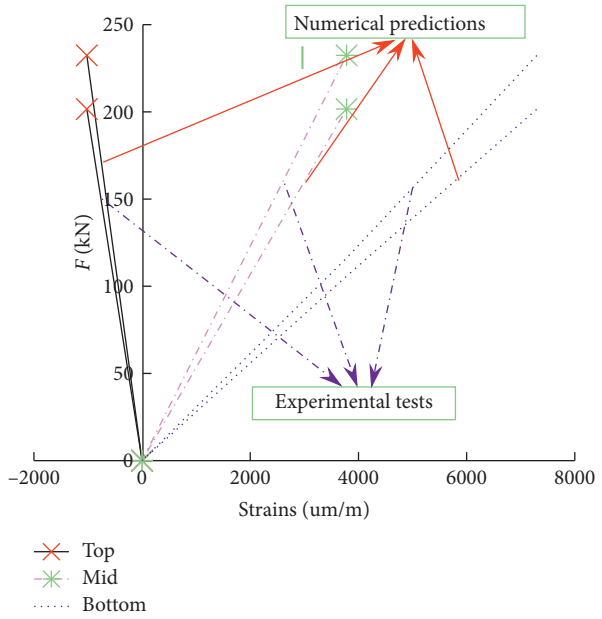

Figure 8: Failure test: mid-span average strains up until failure.

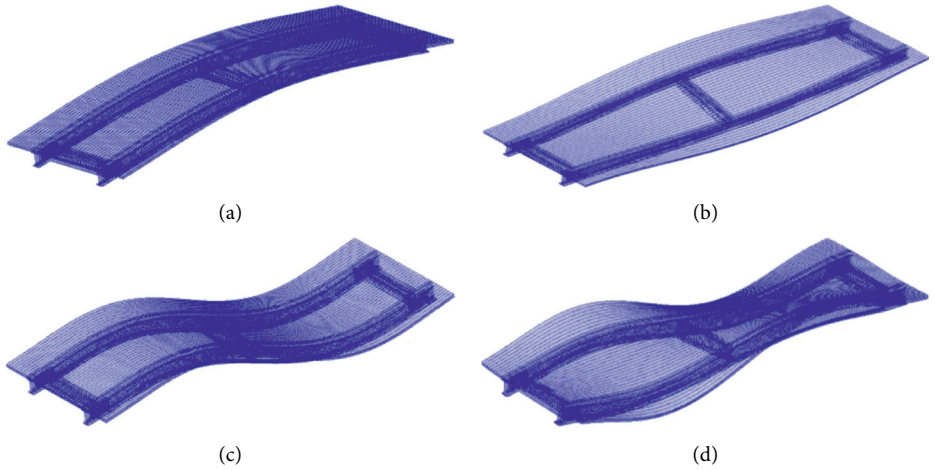

Figure 9: Mode shapes obtained with the FE model predictions. (a) Mode 1. (b) Mode 2. (c) Mode 3. (d) Mode 4.

Table 4: Mode frequencies: experimental results vs numerical predictions.

Mode no.	Shape	Experimental (Hz)	FE model (Hz)
1	Flexure	8.18	7.96
2	Torsion	12.44	14.35
3	Flexure	29.21	27.77
4	Torsion	33.81	35.77

are selected to investigate: (i) corrugated web width, (ii) corrugated web thickness, (iii) SFRSCC concrete slab height, and (iv) corrugated web height.

4.2.1. Effect of Width Variation on the Vibration Frequencies. Based on previous modeling approach, five typical corrugated web width FEA models are built, which use 10 mm, 15 mm, 20 mm, 25 mm, and 30 mm, respectively. Table 7 summarizes natural vibration frequencies with respect to different corrugated web widths in FEA models.

The vibration of flexure and torsion frequencies exert a similar decrease trend from mode shapes 1 to 4 when subjected to increase of corrugated web width. It is observed that the first flexure vibration frequency value decreases 2.5%, 4.5%, 5.8%, and 6.8%, and changing rate tends to diminish. A

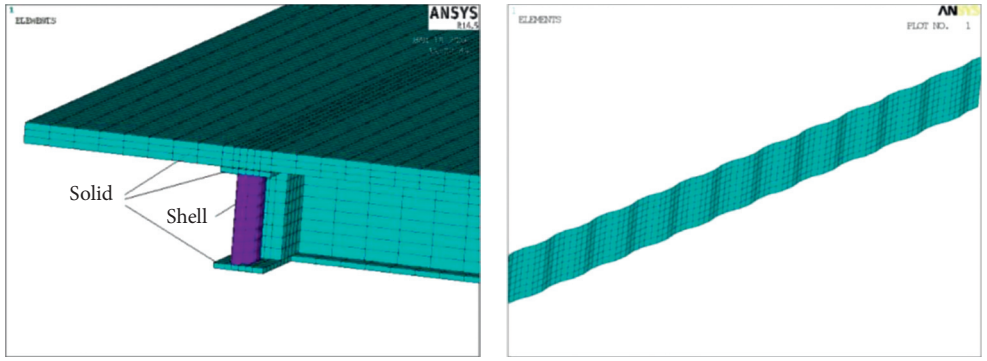

(a) (b)

Figure 10: FE model of the two I-shaped GFRP with corrugated webs-concrete hybrid girder. (a) 3D finite element model. (b) Corrugated web.

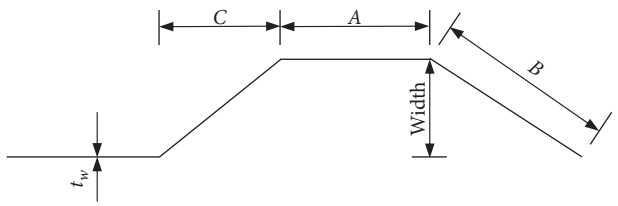

Figure 11: Dimensions of GFRP corrugated steel web.

Table 5: Mode frequencies: FE model (straight webs) vs. FE model (corrugated webs).

Mode no.	Shape	FE model (straight webs) (Hz)	FE model (corrugated webs) (Hz)
1	Flexure	7.96	7.43
2	Torsion	14.35	14.03
3	Flexure	27.77	26.23
4	Torsion	35.77	34.86

Table 6: Mid-span deflection and neutral axis position: FE model (straight webs) vs. FE model (corrugated webs).

Static test	FE model (straight webs)	FE model (corrugated webs)
Mid-span average deflection (mm)	7.24	8.31
Neutral axis position (mm)	31.19	28.93

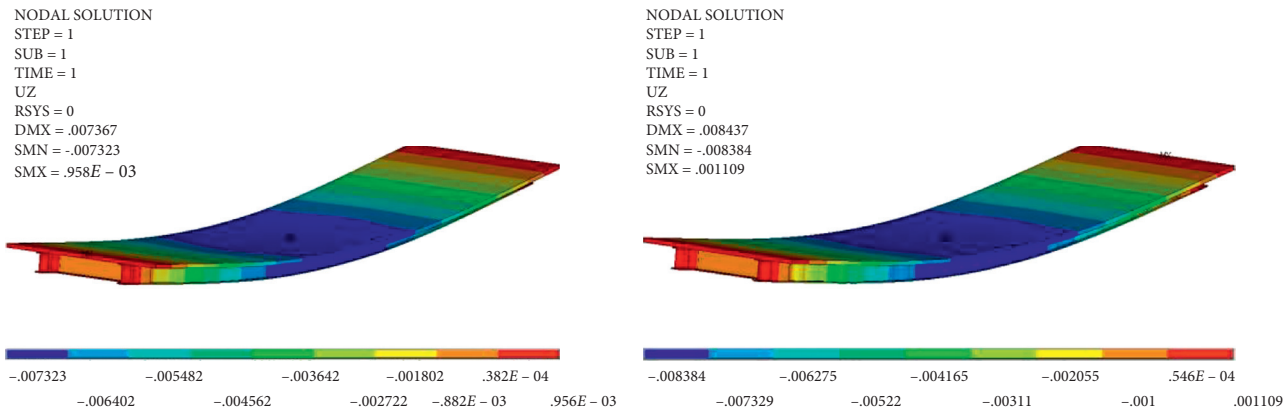

(a) (b)

Figure 12: Mid-span deflections: FE model (straight webs) vs. FE model (corrugated webs). (a) FE model with straight webs. (b) FE model with corrugated webs.

Table 7: Natural vibration frequencies with the width changes.

Mode no.	Shape	Frequencies (Hz) Width				
		10 mm	15 mm	20 mm	25 mm	30 mm
1	Flexure	7.43	7.24	7.09	6.999	6.919
2	Torsion	14.03	13.93	13.82	13.73	13.67
3	Flexure	26.23	25.66	25.21	24.88	24.64
4	Torsion	34.86	34.73	34.42	34.18	33.99

similar situation occurs in second flexure vibration, and variation rates are 2.2%, 3.9%, 5.1%, and 6.1%, respectively. Compared with the variation trend of flexure vibration frequency, two types of torsion vibration frequency show a relatively slow descent trend. The first torsion frequency decreasing rate is 0.7%, 1.5%, 2.1%, and 2.6%, while the second torsion frequency decreasing rate is 0.4%, 1.3%, 2.0%, and 2.5%. All these observations elucidate that variation of corrugated web width may reduce bending and torsional stiffness in two I-shaped GFRP with corrugated webs composite girder system, but the torsion frequency attenuation rate is not evident when compared with flexural frequency.

4.2.2. Effect of Thickness Variation of GFRP Corrugated Web on Natural Frequencies. In order to understand the contribution of GFRP girder web thickness in shear force resistance, three common types of corrugated web thicknesses t_w are selected, which are 5 mm, 10 mm, and 15 mm, respectively. After selection of girder web width and thickness, a total of 15 girder combinations are simulated in dynamic analysis FEA models. The first and second modes of bending and torsion frequencies are shown in Figure 13.

The effect of corrugated web width is firstly considered in model vibration frequency. Both bending and torsion frequency values have an insignificant influence for 5 mm corrugated web thicknesses, although corrugated web width varies from 10 to 30 mm. For 10 mm corrugated web thickness, ultimately bending and torsion frequencies decrease rates are 6.1% and 2.5% when corrugated web width ranges from 10 to 30 mm. The variation trend turns more obvious in 15 mm web thickness, and the variation rates of 9.4% and 4.4% are observed for bending and torsion frequencies. In addition, the influence of corrugated web thickness in model vibration frequency is investigated. The first and second order of bending frequencies showed an average increase of 9.1% and 16.8% when corrugated web thickness ranged from 5 mm to 15 mm, respectively. Similarly, the corresponding torsional frequencies exhibited an increase of 8.1% and 14.2%, respectively. These observations are attributed to the fact that increase of corrugated web thickness is more helpful than corrugated web width variation to improve the dynamic performance of corrugated webs composite girder system.

4.2.3. Effect of the Height Variation of the Concrete Top Slab on the Natural Frequencies. As the major compression member in GFRP composite girder system, SFRSCC concrete slab height is an important factor in structure design. Beyond that, steel anchor bolts connecting GFRP girder and concrete slab also need enough anchorage lengths. Based on the above requirements, three concrete top slab heights h_c are chosen to investigate, which are 20 mm, 40 mm, and 60 mm, respectively. Figure 14 shows the first and second mode of bending and torsion frequency distribution with respect to concrete top slab height h_c varies, and influence of GFRP girder web width is also considered.

It can be seen that bending frequency exerts a descent trend with increasing of concrete top slab height, not related to the variation of GFRP web width; however, the torsional frequency variation follows the contrary way. The first and second bending frequency show relatively consistent decay rates of 18% and 15%, respectively. On the contrary, first and second torsional frequency of the largest concrete top slab height ($h_c = 60$ mm) resulted in ultimately 27% and 29% higher growth rate than those of $h_c = 40$ mm (5.3% and 13.4%). Furthermore, a variation of web width for the same slab height has an insignificant influence on bending and torsion frequency values. It should be noted that increase of concrete slab height is only helpful for torsion vibration frequencies, but weakens bending vibration frequencies. Thus, it is proved that adjustment of concrete top slab height h_c is only a partial effective way to improve dynamic characteristics for GFRP composite girder system.

4.2.4. Effect of the Height of GFRP Corrugated Web on Natural Frequencies. Generally, girder web height plays a major role in determining structure dynamic performance. Thus, three types of GFRP corrugated web height are selected to investigate the influence of vibration frequencies, which are 200 mm, 300 mm, and 400 mm, respectively. The model vibration (bending and torsion) frequencies for different web height and width are obtained and comparison analysis is shown in Figure 15.

As expected, the higher web height leads to larger first and second mode vibration (bending and torsion) frequency values. Among the variation of frequency, the first mode bending frequency ascent trend is more evident than other modes' frequency, separately increasing 38.1% for 300 mm web height and 73.8% for 400 mm web height when compared with 200 mm web height model. Similarly, second bending frequency exerts a 27.2% and 46.0% ascent trend with respect to 300 mm and 400 mm corrugated web height, respectively. For first and second mode torsion

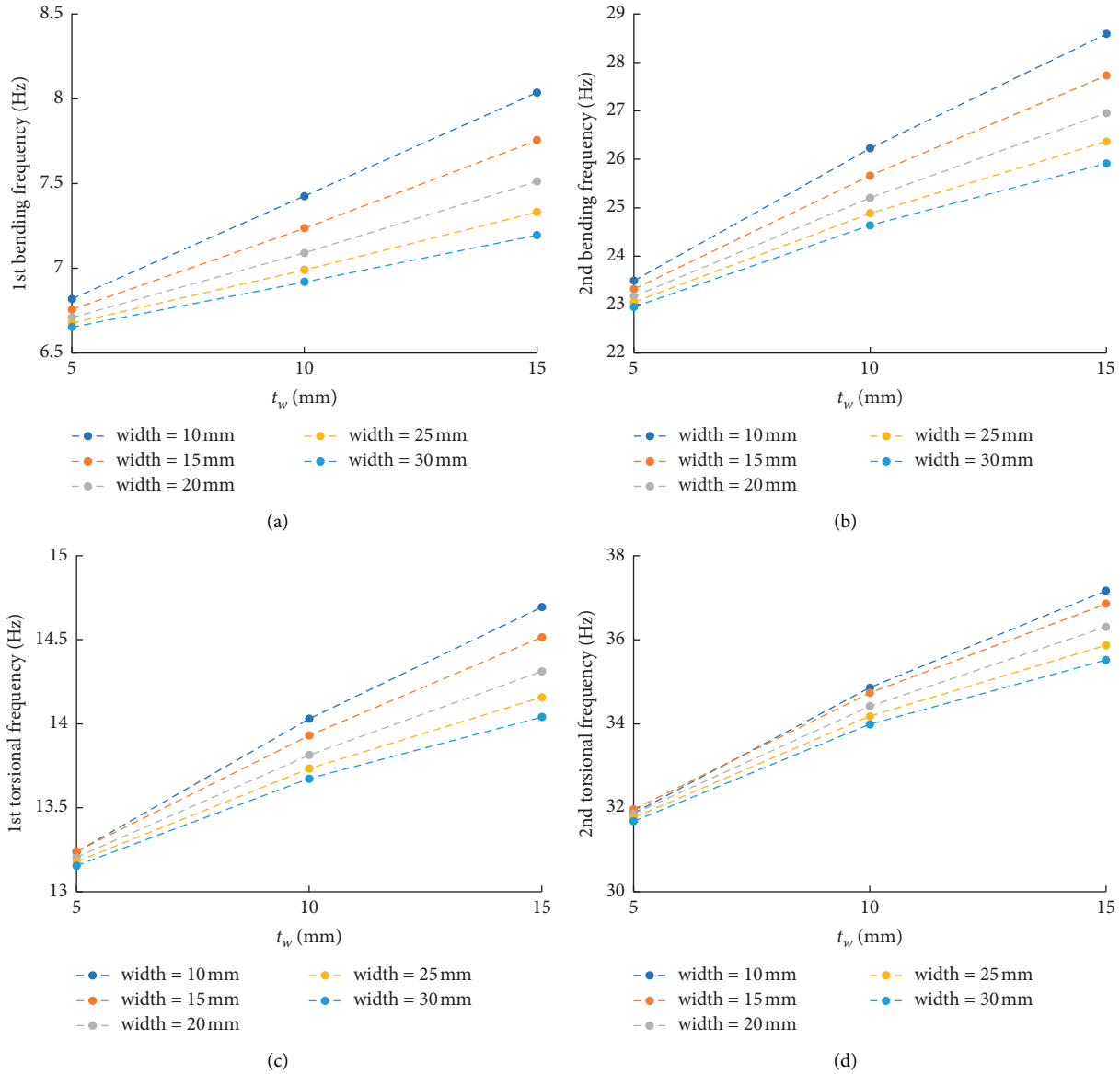

Figure 13: Natural vibration frequencies with t_w changes.

frequency, results show on average a steady ascent rate of 40.4% and 34.6% due to web height increasing 1.5 and 2 times. Beyond that, the influence of web width is also considered when subjected to web height variation. The variation trend is not obvious, and the maximum changing rate is only 6.8% that occurred in first bending vibration. Thus, it can be observed that height of corrugated web (h_g) is a very sensitive factor in dynamic characteristics of two I-shaped GFRP with corrugated web composite girder system.

The objective of parameters study is to estimate the efficacy of each parameter in structure dynamic performance. It can be concluded that corrugated web height is the most efficient factor to increase the structure bending and torsion frequency, but it also needs to follow design requirements like depth-width ratio or depth-thickness ratio. Furthermore, the static performance is also considered with the variation of four parameters. As an important index, maximum vertical deflection subjected to parameter variation is investigated with static load condition, as shown in Figure 5.

5. Parameter Analysis of Deflection

The four-parameter (corrugated web width, corrugated web thickness, SFRSCC concrete slab height, and corrugated web height) mid-span deflection result is shown in Figure 16.

An interesting observation is that only corrugated web width exerted a positive correlation with girder mid-span deflection; however, an inverse correlation occurs for all other three parameters, including corrugated web thickness t_w, concrete top slab h_c, and corrugated web height h_g. In addition, the influence of each parameter dimension

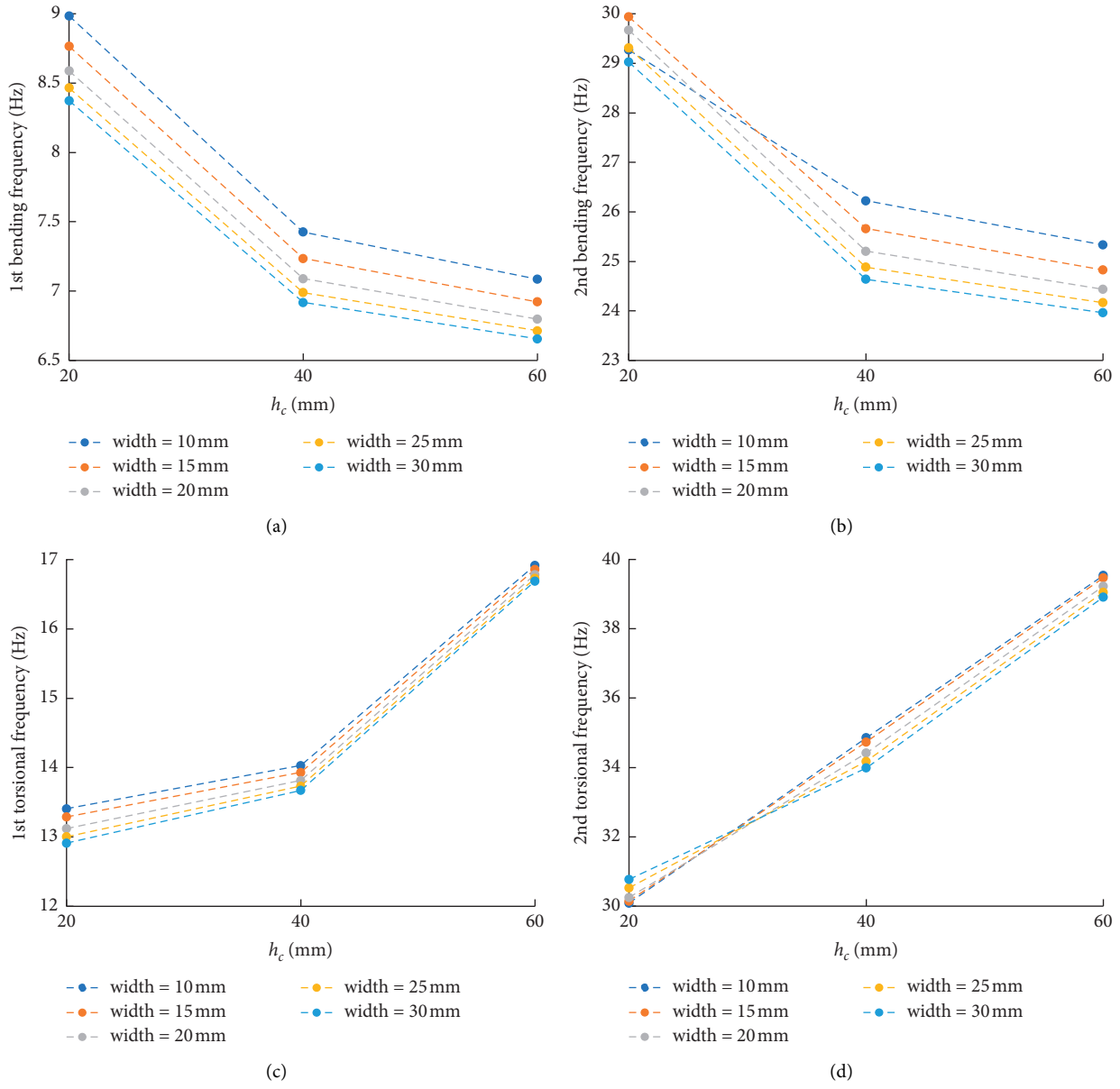

Figure 14: Natural vibration frequencies with h_c changes.

variation in mid-span deflection is different, such as only 15% increasing of mid-span deflection when corrugated web width varies from 10 mm to 30 mm. It can be explained that increase of corrugated web width is not helpful to improve vertical stiffness when subjected to vertical static loading. An approximately linear descent trend is observed with the increase of corrugated web thickness and concrete top slab, which shows ultimately 24.2% and 40.8% decreasing of mid-span deflection, respectively. The effect of corrugated web height plays a more sensitive role in mid-span deflection and resists 70.7% deformation when web height changes from 200 mm to 400 mm. All these observations proved that corrugated web height is the most efficient way to improve the vertical stiffness and resist the deformation of GFRP corrugated webs-concrete composite girder system.

6. Wind Load Effect on the Deflection

In addition to the vertical load, the influence of lateral load effect, especially wind load, also needs to be evaluated in two I-shaped GFRP with corrugated webs-concrete composite girder bridge. In this research, the most unfavorable wind load, 50 psf, is considered in FEA model, based on AASHTO FRP pedestrian bridge design code [26]. The wind pressures (modeled as uniform load) are loaded on one whole side face of a girder corrugated web, as shown in Figure 17(a). It can be seen that larger deformation location of corrugated web girder appears in the bottom of 1/4 span and 3/4 span because of symmetric geometric dimension, as shown in Figure 17(b).

This observation can explain that the secondary girders exist in both end and mid-span location, which can resist partial

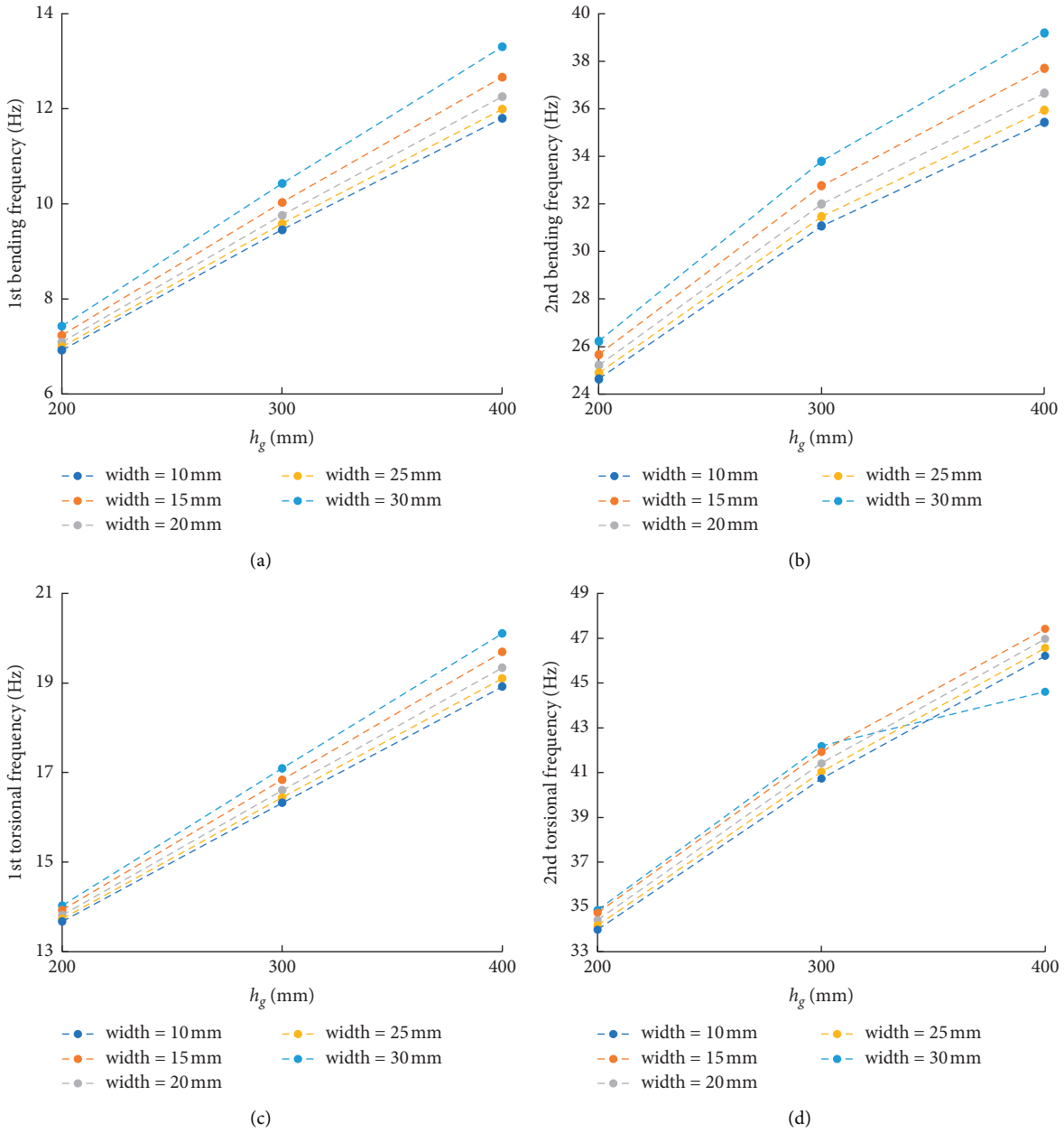

Figure 15: Natural vibration frequencies with h_g changes.

torsional deflection and SFRSCC concrete slab and also effectively prevent the girder top deformation. Further discussions on the influence of corrugated web width, thickness t_w, height h_g, and concrete slab thickness h_c when subjected to the same wind load condition, and the comparison results are shown in Figure 18.

The structure lateral flexural behavior affected by four parameters is inconsistent and needs to be discussed separately. With increasing of corrugated web width, thickness, and concrete slab thickness, the maximum lateral displacement appears to have a similar descent trend, whereas corrugated web height has an opposite trend. A similar descent trend is observed in Figure 18 for three parameters, which averagely decreases 43% for corrugated web width, 46.6% for corrugated web thickness, and 65.8% for concrete slab thickness. Furthermore, the increase of corrugated web height leads to ultimately 6.9 times when compared with initial lateral displacement. Compared with other three parameters, corrugated web height is the most sensitive parameter with the effect of wind load. Thus, these observations imply that increasing of corrugated web width, corrugated web thickness t_w, and concrete slab thickness h_c helps to improve the transverse stability of structure with respect to lateral load, but the effect of corrugated web height is on the contrary.

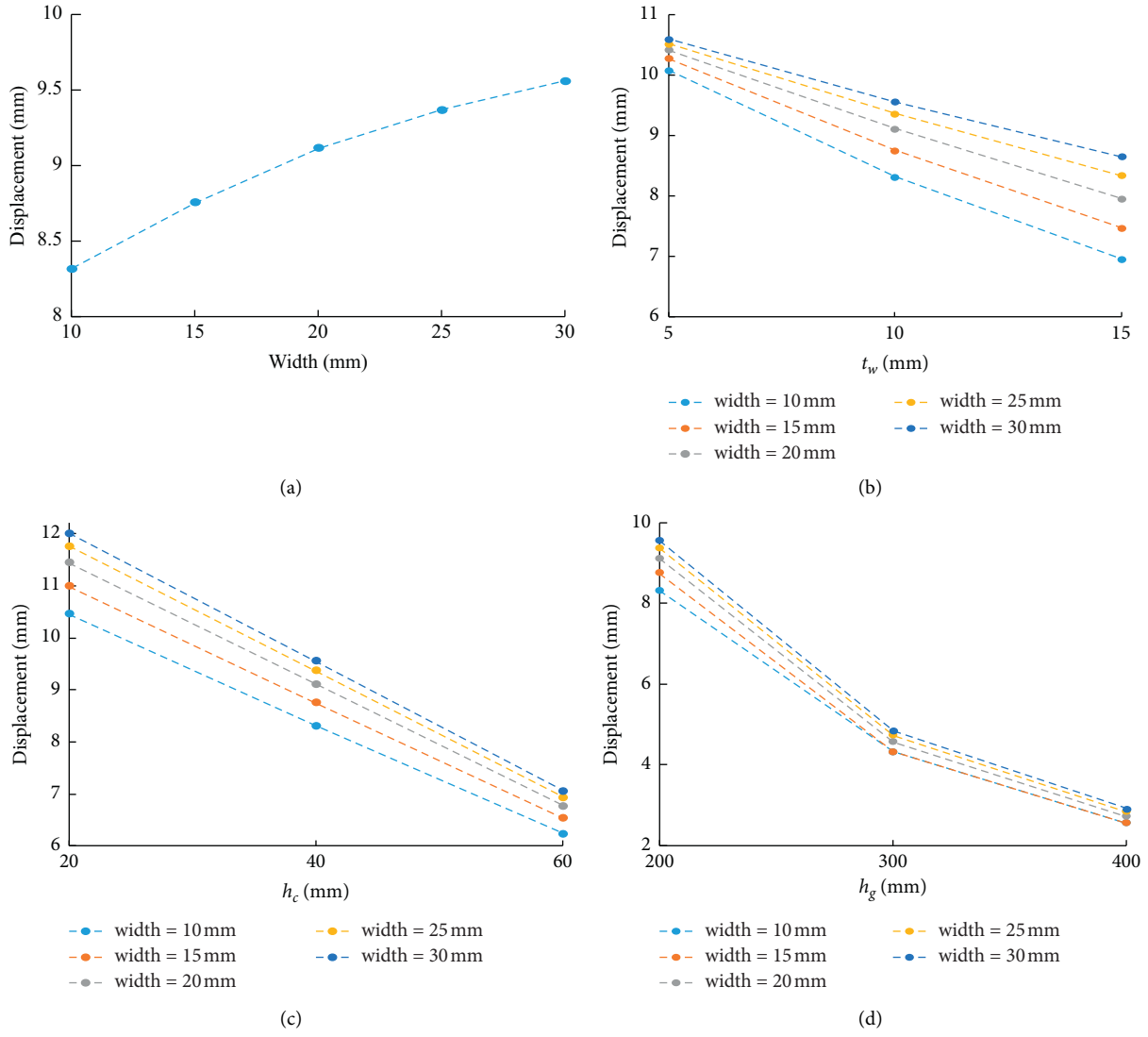

Figure 16: Displacement of the two I-shaped GFRP with corrugated webs-concrete hybrid girder.

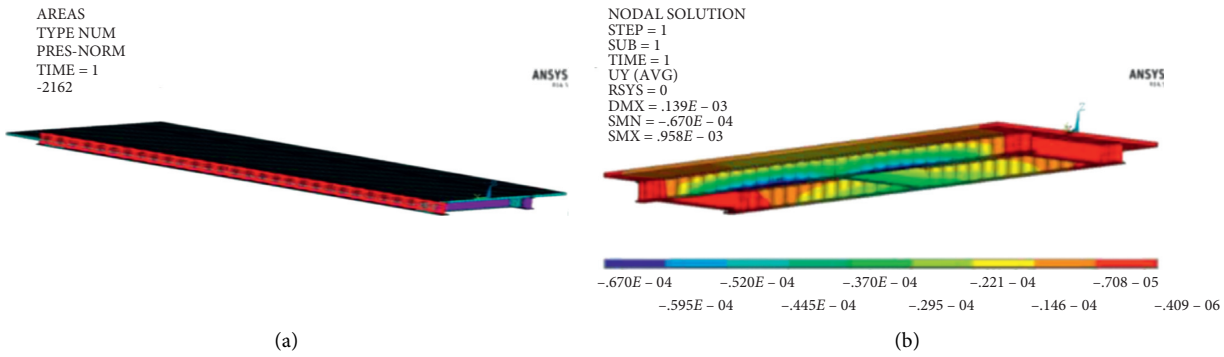

Figure 17: Wind load on the two I-shaped GFRP with corrugated webs-concrete hybrid girder. (a) Wind load action. (b) Displacement contour under wind load action.

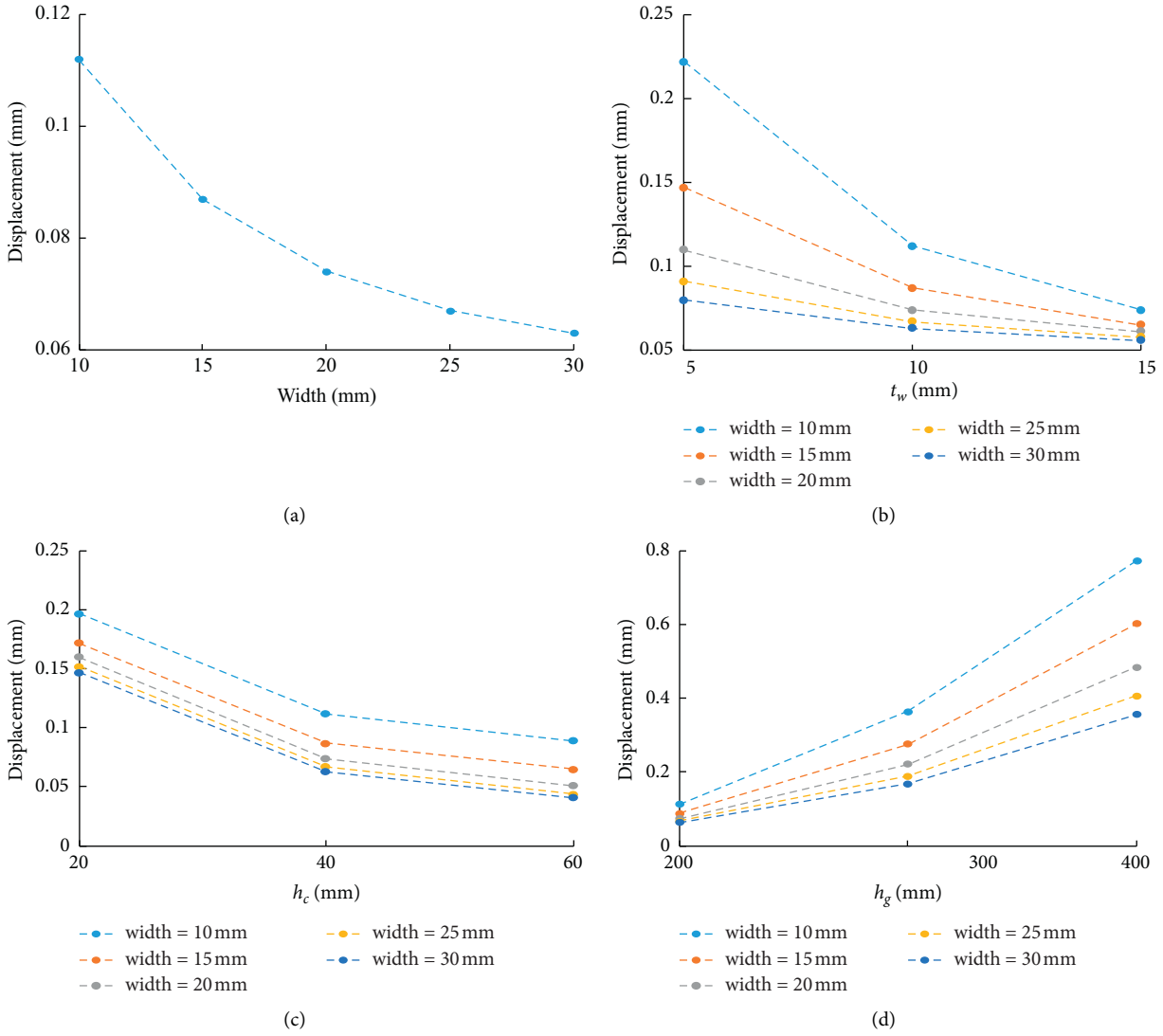

Figure 18: Lateral displacement of the two I-shaped GFRP with corrugated webs-concrete hybrid girder.

7. Conclusions

This paper studies the static and dynamic behavior of the two I-shaped GFRP composite girders with corrugated and straight webs bridge, respectively. A three-dimensional FEA model is developed and validated by experimental data. The following main conclusions are drawn:

(1) The FEA model simulation result shows improvement of shear stability when straight webs are replaced by the corrugated webs in GFRP-concrete composite girder system, however, accompanied by bending and torsion frequencies decrease in a certain degree. Beyond that, it also leads to increase of maximum vertical deflection, and neutral axis position moves towards the top concrete slab, but is not so obvious.

(2) Girder corrugated web width has a little influence on the vibration (bending and torsion) frequencies, while corrugated webs thickness t_w, concrete slab height h_c, and corrugated webs height h_g have more obvious influences on that. With the increase of corrugated webs width, the vibration frequencies decrease, whereas t_w and h_g exert an opposite trend. Considering concrete slab thickness increases, the bending and torsional vibration frequencies reveal a reverse varying trend: bending vibration frequencies descend, while the torsion vibration frequencies ascend.

(3) Considered the maximum vertical deflection in midspan, it shows a slow increase trend followed by increasing of corrugated web width. However, it exerts a noticeable decrease trend with increasing of corrugated web thickness, height, and concrete slab thickness.

(4) Lateral load influence of structure is investigated when subjected to wind load. With the increase of GFRP corrugated web width, lateral displacement shows an increasing trend, whereas an opposite trend is observed with corrugated web thickness, height, and concrete slab thickness. These trends imply that

the growth of GFRP corrugated web thickness, height, and the concrete slab thickness is helpful to improve transverse stability in two I-shaped GFRP with corrugated webs-concrete composite girder bridge.

Data Availability

The data used to support the findings of this study are available from the corresponding author upon request.

Conflicts of Interest

The authors declare that they have no conflicts of interest.

Acknowledgments

This work was supported partially by two grants from Scientific Research Project of Department of Housing and Urban-Rural Development of Gansu Province (Grant nos. JK2018-46 and JK2020-21) and partially by the Key Research and Development Program of Gansu Province (20YF3FA039).

References

[1] N. D. Hai, H. Mutsuyoshi, S. Asamoto, and T. Matsui, "Structural behavior of hybrid FRP composite I-beam," *Construction and Building Materials*, vol. 24, no. 6, pp. 956–969, 2010.

[2] F. K. Ilker and F. A. Ashraf, "Moment redistribution in continuous FRP reinforced concrete beams," *Construction and Building Materials*, vol. 49, no. 12, pp. 939–948, 2013.

[3] Y. J. Kim and A. Fam, "Numerical analysis of pultruded GFRP box girders supporting adhesively-bonded concrete deck in flexure," *Engineering Structures*, vol. 33, no. 12, pp. 3527–3536, 2011.

[4] M. Al-Rubaye, A. Manalo, O. Alajarmeh et al., "Flexural behaviour of concrete slabs reinforced with GFRP bars and hollow composite reinforcing systems," *Composite Structures*, vol. 236, Article ID 111836, 2020.

[5] A. A. Mohammed, A. C. Manalo, W. Ferdous, Y. Zhuge, P. V. Vijay, and J. Pettigrew, "Experimental and numerical evaluations on the behaviour of structures repaired using prefabricated FRP composites jacket," *Engineering Structures*, vol. 210, Article ID 110358, 2020.

[6] A. Siddika, M. A. A. Mamun, W. Ferdous, and R. Alyousef, "Performances, challenges and opportunities in strengthening reinforced concrete structures by using FRPs-a state-of-the-art review," *Engineering Failure Analysis*, vol. 111, Article ID 104480, 2020.

[7] L. C. Bank, *Hybrids for Construction: Structural Design with FRP Materials*, J Wiley & Sons, Hoboken, NJ, USA, 2006.

[8] T. Keller and J. de Castro, "System ductility and redundancy of FRP beam structures with ductile adhesive joints," *Composites Part B: Engineering*, vol. 36, no. 8, pp. 586–596, 2005.

[9] J. R. Correia, F. A. Branco, N. M. F. Silva, D. Camotim, and N. Silvestre, "First-order, buckling and post-buckling behaviour of GFRP pultruded beams. part 1: experimental study," *Computers and Structures*, vol. 89, no. 21-22, pp. 2052–2064, 2011.

[10] N. M. F. Silva, D. Camotim, N. Silvestre, J. R. Correia, and F. A. Branco, "First-order, buckling and post-buckling behaviour of GFRP pultruded beams. part 2: numerical simulation," *Computers and Structures*, vol. 89, no. 21-22, pp. 2065–2078, 2011.

[11] J. R. Correia, F. A. Branco, and J. Ferreira, "GFRP-concrete hybrid cross-sections for floors of buildings," *Engineering Structures*, vol. 31, no. 6, pp. 1331–1343, 2009.

[12] M. N. Fardis and H. Khalili, "Concrete encased in fiberglass-reinforced plastic," *ACI Journal Proceedings*, vol. 78, no. 6, pp. 440–446, 1981.

[13] A. Fam, D. Schnerch, and S. Rizkalla, "Rectangular filament-wound glass fiber reinforced polymer tubes filled with concrete under flexural and axial loading: experimental investigation," *Journal of Composites for Construction*, vol. 9, no. 1, pp. 25–33, 2005.

[14] A. Fam and H. Honickman, "Built-up hybrid composite box girders fabricated and tested in flexure," *Engineering Structures*, vol. 32, no. 4, pp. 1028–1037, 2010.

[15] R. C. João, F. A. Branco, and J. G. Ferreira, "Flexural behaviour of GFRP-concrete hybrid beams with interconnection slip," *Hybrid Structures*, vol. 77, no. 1, pp. 66–78, 2007.

[16] R. C. João, F. A. Branco, and J. G. Ferreira, "Flexural behaviour of multi-span GFRP-concrete hybrid beams," *Engineering Structures*, vol. 31, no. 7, pp. 1369–1391, 2009.

[17] P. J. D. Mendes, J. A. O. Barros, J. Sena-Cruz, and M. Teheri, "Influence of fatigue and aggressive exposure on GFRP girder to SFRSCC deck all-adhesive connection," *Composite Structures*, vol. 110, pp. 152–162, 2014.

[18] J. A. Gonilha, J. R. Correia, F. A. Branco, E. Caetano, and Á. Cunha, "Modal identification of a GFRP-concrete hybrid footbridge prototype: experimental tests and analytical and numerical simulations," *Composite Structures*, vol. 106, pp. 724–733, 2013.

[19] J. A. Gonilha, J. R. Correia, and F. A. Branco, "Structural behaviour of a GFRP-concrete hybrid footbridge prototype: experimental tests and numerical and analytical simulations," *Engineering Structures*, vol. 60, pp. 11–22, 2014.

[20] J. A. Gonilha, J. Barros, J. R. Correia et al., "Static, dynamic and creep behaviour of a full-scale GFRP-SFRSCC hybrid footbridge," *Composite Structures*, vol. 118, pp. 496–509, 2014.

[21] J. A. Gonilha, J. R. Correia, and F. A. Branco, "Dynamic response under pedestrian load of a GFRP-SFRSCC hybrid footbridge prototype: experimental tests and numerical simulation," *Composite Structures*, vol. 95, pp. 453–463, 2013.

[22] J. A. Gonilha, J. R. Correia, and F. A. Branco, "Creep response of GFRP-concrete hybrid structures: application to a footbridge prototype," *Composites Part B: Engineering*, vol. 53, pp. 193–206, 2013.

[23] R. Sause and T. N. Braxtan, "Shear strength of trapezoidal corrugated steel webs," *Journal of Constructional Steel Research*, vol. 67, no. 2, pp. 223–236, 2011.

[24] S. Zangana, J. Epaarachchi, W. Ferdous, and J. Leng, "A novel hybridised composite sandwich core with glass, kevlar and zylon fibres-investigation under low-velocity impact," *International Journal of Impact Engineering*, vol. 137, Article ID 103430, 2020.

[25] EN 1994-1-1, *Eurocode 4: Design of Hybrid Steel and Concrete Structures-Part 1-1: General Rules and Rules for Buildings*, European Committee for Standardization (CEN), Brussels, Belgium, 2004.

[26] AASHTO, *Guide Specifications for Design of FRP Pedestrian Bridges*, American Association of State Highway and Transportation Officials, Washington. DC, USA, 2008.